Est. 1984

ORIENTAL JOURNAL OF CHEMISTRY
An International Open Access, Peer Reviewed Research Journal

www.orientjchem.org

ISSN: 0970-020 X
CODEN: OJCHEG
2023, Vol. 39, No.(2):
Pg. 222-230

Ferrocenyl Hydroxy Methyl Coupled Caffeine Synthesis, Density Functional Theory, ADME Prediction and Docking Analysis of It's Binding Interactions to Coronavirus Main Protease

SONDOS ABDULLAH J ALMAHMOUD[1], MICHELE CARIELLO[2] and AMIN OSMAN ELZUPIR[1]*

[1]Department of Chemistry, College of Science, Imam Mohammad Ibn Saud Islamic University (IMSIU), Riyadh 11623, Saudi Arabia.
[2]School of Chemistry, University of Glasgow, Glasgow, G12 8QQ, United Kingdom.
*Corresponding author E-mail: aoalamalhuda@imamu.edu.sa

http://dx.doi.org/10.13005/ojc/390201

(Received: March 24, 2023; Accepted: April 25, 2023)

ABSTRACT

The COVID-19 pandemic has made the world aware of how crucial the development of cost-effective and scalable antiviral drugs is. Here we report the synthesis of caffeine-based 8-[(ferrocenyl)(hydroxy)methyl]-1,3,7-trimethyl-3,7-dihydro-1H-purine-2,6-dione (FHC), and its use as an inhibitor of protease (M^{pro}), an essential enzyme for SARS-CoV-2 viral replication. FHC was modelled through density functional theory to get an insight of its properties, and fully characterized through conventional techniques. Its activity against M^{pro} was investigated using a molecular docking approach, showing excellent binding affinity to the catalytic dyad of His41 and Cys145 and the active sites of M^{pro} with energies score ranging from –6.7 to –7.0 kcal/mol. The affinity of conformers to bind to the active pocket was 44%. Based on a detailed investigation, it appears that FHC has a safe ADME profile, and that it could be a potential inhibitor for M^{pro} of SARS-CoV-2.

Keywords: Caffeine, Ferrocene, Coronavirus, DFT, ADME, Molecular docking.

INTRODUCTION

Naturally abundant caffeine (1,3,7-trimethylxanthine) is the most widely consumed psychostimulant drug worldwide. Due to its many therapeutic properties, caffeine is considered as a unique compound in the field of medicinal chemistry. The attention of the scientific community towards caffeine is due to its ability to comply with the rule of five, including the moderate lipophilicity (experimental logP–0.01, other sources logP–0.07), and to cross biological membranes/barriers, together with the high solubility in water.[1-6] There are several reviews in the literature covering the therapeutic applications of caffeine and its derivatives.[1,7-13] The antiviral activities of caffeine were reported in several preliminary studies against different viruses, such as influenza virus, poliovirus, herpes simplex virus (HSV-1)

and vaccinia virus.[14-15] Another study reported the inhibition of the viral protein synthesis by caffeine and the suppression of the plaque formation of HSV-1 by interfering with the cell-to-cell transmission of the virus.[15] It was found that Poliovirus and HSV-1 replication are sensitive to caffeine, suggesting that caffeine can indeed inhibit both DNA and RNA viruses.[16] Due to the role it can play against different viruses, caffeine has recently attracted considerable attention for the SARS-CoV-2 treatment.[9,17-18]

Moreover, the organometallic compound ferrocene (Fc) is one of the most studied scaffolds with numerous uses in various fields of chemistry such as material science, catalysis, diagnostic applications and medicinal as well as synthetic fields.[19-25] The unique structure of Fc, featuring an iron metal sandwiched between two (Cp) rings leads to the electron donating ability of Fc which results in several chemical properties such as the ease of reversable oxidation to ferricenium ions, the high reactivity in electrophilic substitution reactions and the ease of functionalization.[26, 27] Fc also shows lipophilic and non-toxic properties, good solubility in most of common organic solvents, stability in aerobic and aqueous media, good air and thermal stability up to 400.[28] Taking the aforementioned exceptional properties into consideration, Fc-based biological and medicinal applications have attracted considerable attention and its derivatives have been shown to have many biological activities, such as DNA-cleavage, antibacterial, antifungal, antiparasitic and anticancer drug candidates.[29-36] Ferrocene conjugates were studied for their potential activity against other viruses such as human immunodeficiency viruses (HIV), which lead to acquired immunodeficiency syndrome AIDS, and the hepatotropic RNA virus hepatitis C virus (HCV).[37-39] The fact that Fc groups possess lipophilicity facilitates its penetration through cellular and nuclear membranes.[24]

SARS-CoV-2 is a beta coronavirus of group 2B with over 70% genetic sequence similarity to that of SARS-CoV-1.[7,40] SARS-CoV-2 has shown a higher infection rate and a more extended incubation period, as compared to previous coronaviruses such as Middle East respiratory syndrome coronavirus.[41] Thus, it has become crucial for medicinal chemists to develop strategic research plans to produce anti-viral drugs for COVID-19 treatment. There are two enzymes that control proteolysis, the coronavirus main protease (M^{pro}) and the papain-like protease (PL^{pro}).[42] Since the Mpro enzyme, also called $3CL^{pro}$, is essential to the viral replication and infection process, it has been considered as an ideal target for antiviral therapy.[43-45]

Our previous study showed the ability of caffeine and its derivatives to function as inhibitor against M^{pro} with binding affinity score ranging from –4.9 to –8.6 kcal/mol.[18] Among the investigated drugs, caffeine showed a high binding affinity via hydrogen bonding to Glu 166 and Cys 145, with a relatively high binding percentage (67%) and low RMSD value. Further, the inhibitory activity of M^{pro} with 42 pyrimidonic pharmaceuticals were also investigated.[46] The study revealed that the high molecular weight drugs interact poorly to the active site of M^{pro}, whereas the low molecular weight drugs interact with poor binding energy. Taking this balance into account, we designed and sinthesized a new biologically active caffeine containing drug and studied its potential as a therapeutic candidate against M^{pro} of SARS-CoV-2 by molecular docking studies. Our design combines caffeine with the well-known biologically active Fc moiety.

MATERIALS AND METHODS

Synthesis of 8-[(Ferrocenyl)(hydroxy)methyl]-1,3,7-trimethyl-3,7-dihydro-1H-purine-2,6-dione (FHC)

Ferrocenecarboxaldehyde (0.100 g, 0.467 mmol), caffeine (90.7 mg, 0.467 mmol) and sodium hydroxide (2.00 g) were dissolved in dimethyl sulfoxide (30 mL) and the mixture was stirred at 90°C for 4 hours. The completion of reaction was monitored by RP-HPLC-UV. The reaction mixture was allowed to cool to room temperature, neutralized to pH 7 using concentrated hydrochloric acid, then poured into acetonitrile (60 mL). The formed dark precipitate was collected by filtration, washed with acetonitrile, and left to dry in air to give the title compound as a dark brown solid (190 mg, 65%). Mp>300°C. ^{1}H NMR (D_2O, 400 MHz, Me_4Si) δ 2.66 (m, 9H, CH_3), 4.77 (s, 11H, overlapped with the solvent peak). HR-MS: M/z (M^+=408.3735). FTIR λ_{max} 3334 cm^{-1} (OH). λ_{max} (water, 291nm).

Computational details

Density functional theory (DFT) calculations were performed using Gaussian 09 software suite.[47] The system was geometrically optimized, using the B3LYP functional, and a mixed basis set, which includes the 631++G(d,p) for every atom except Fe, for which a LanL2DZ basis set was employed. A further frequency calculation was run to ensure no negative IR frequencies were present. The NMR spectrum was simulated in water using the mixed basis set: 6311G+(2d,p)/LanL2DZ. TMS, calculated at the same level of accuracy was used as a reference. A TD-DFT calculation, using a CAM-B3LYP functional and the same basis set employed for the ground state calculation, was performed to determine the frontier molecular orbitals of FHC and to determine the UV-Vis absorption spectrum in water.

Molecular docking

The M^{pro} crystal structure was obtained from the Protein Data Bank (PDB ID: 6Y2E). The water molecules were removed, missing hydrogens atoms were added, and minimized to its lower energy conformation.[46] The net charge was calculated using antechamber, and its energy was minimized using Molecular Modelling Toolkit plugin UCSF Chimera. The AutoDock Vina has been used to perform docking with grid box size of (29.08, 58.58, 57.04) Å, cantered at (–16.19× –26.14×17.46) Å. UCSF Chimera was used for visualization of bonds interactions and images processing.[46]

RESULTS AND DISCUSSION

Synthesis

The synthesis of the target compound FHC is shown in Scheme 1. FHC was synthesised via the reaction of commercially available compound ferrocenecarboxaldehyde with caffeine in the presence of an excess amount of sodium hydroxide (NaOH). NaOH was aimed to deprotonate the caffeine creating the anionic derivative which, in turn, attacks the electrophilic carbonyl of ferrocenecarboxaldehyde. FHC was obtained in 65% yield and was characterized using FT-IR, HR-MS and ^{1}H-NMR techniques. Since FHC is only soluble in water, ^{1}H-NMR spectrum (Fig. 1) was recorded in D_2O. The spectrum shows two main broad singlets peaks at chemical shifts of 2.66 and 4.77 ppm. The peak at 2.66 ppm was assigned to the protons of the methyl groups while the peak at 4.77 ppm was assigned to the protons of cyclopentadienyl (Cp) of the Fc which are overlapping with the solvent residue peak. The main important indication of the successful substitution is the disappearance of the caffeine aromatic peak which was reported to appear at 7.58 ppm.[48] Although the hydroxyl proton (-OH) was not confirmed by ^{1}H-NMR as expected due to proton exchange with D_2O, FT-IR spectrum (Fig. 2) shows the presence of a broad stretch band from 2904-3672 cm^{-1} which was assigned to the OH group. TOF-MS using positive and negative ionization mode of electrospray is shown in Fig. 3. The TOF-MS spectrum indicates the presence of the weak parent molecular peak with M of m/z 408.3736, as well as M^+ using the positive mode (Fig. 3(a)) while the negative mode MS spectra shows a strong M^- of m/z 407.1982 (Fig. 3(b)). The UV-Vis absorption spectrum (Fig. 4) shows a wide absorption band in the UV region from 283 nm to 400 nm with a maximum absorption λ_{max} at 291 nm. The optical band gap of FHC is 2.6 eV which was calculated from λ_{onset} (481 nm).

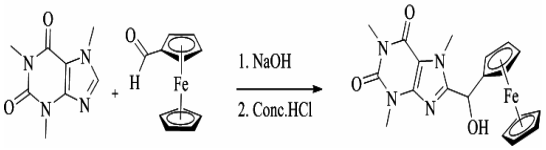

Scheme 1. Synthetic route of the target compound FHC

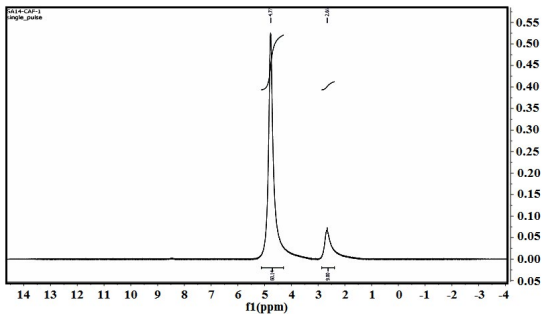

Fig. 1. ^{1}H-NMR spectrum of FHC

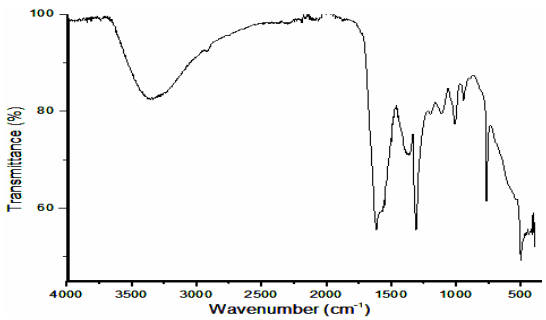

Fig. 2. FT-IR spectrum of FHC

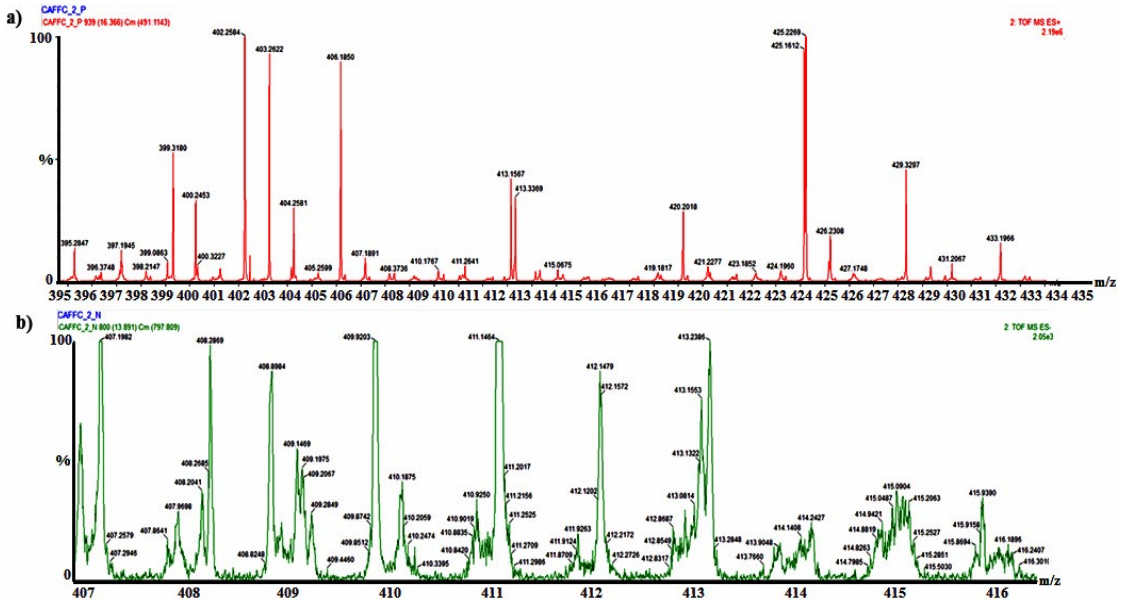

Fig. 3. TOF-MS spectrum of FHC (a) positive mode and (b) negative mode

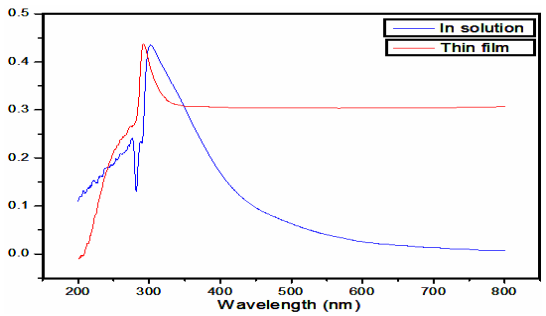

Fig. 4. UV-Vis spectrum of FHC recorded in solution (10^{-5} M in water) and thin film

Theoretical studies

In order to gain insight into the electronic structural properties of FHC, Density Functional Theory (DFT) calculations were conducted. The geometrically optimized structure of FHC (Fig. 5) was calculated using the B3LYP functional, and a mixed basis set, which includes the 631++G(d,p) for every atom except Fe, for which a LanL2DZ basis set was employed. A further frequency calculation was run to ensure the absence of negative IR frequencies. As shown in Fig. 5, the caffeine and the Cp units of the ferrocene lay on orthogonal planes (dihedral angle of 89.3°), likely due to the presence of the sp3 carbon that breaks the conjugation between the two units.

A TD-DFT calculation, at the same accuracy level, was performed to determine the frontier molecular orbitals of FHC. Both, the highest occupied molecular orbital (HOMO) and the lowest unoccupied molecular orbital (LUMO) lay over the caffeine unit (Fig. 6) Their values are –6.16 eV for the HOMO and –1.53 eV for the LUMO, corresponding to a calculated energy gap of 4.63 eV.

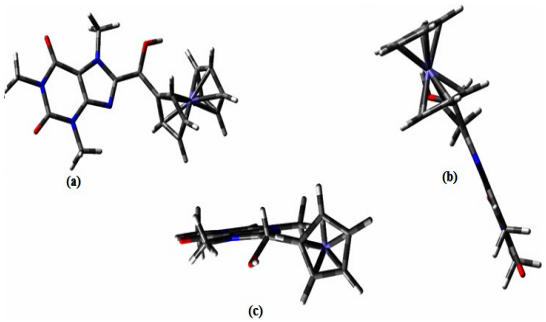

Fig. 5. Optimized ground state geometries of FHC from 3 different angles

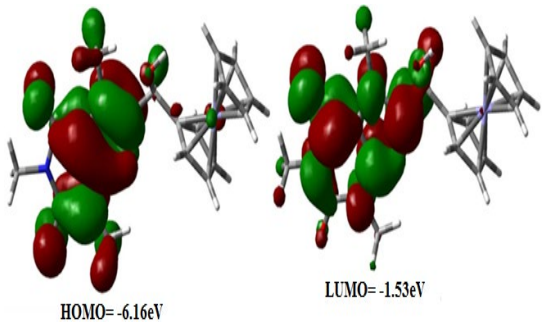

Fig. 6. The highest occupied molecular orbital (HOMO) and the lowest unoccupied molecular orbital (LUMO) of FHC

The NMR spectrum was simulated in water using the mixed basis set: 6311G+(2d,p)/LanL2DZ. TMS, calculated at the same level of accuracy was used as a reference. Due to the rigidity introduced by the geometry optimization, the model does not take into account the rotational averaging of chemically equivalent protons, which could be represented by different chemical shifts. For this reason, their chemical shifts were averaged and reported in Table 1, with atom labels reported as indicated in Figure 7.

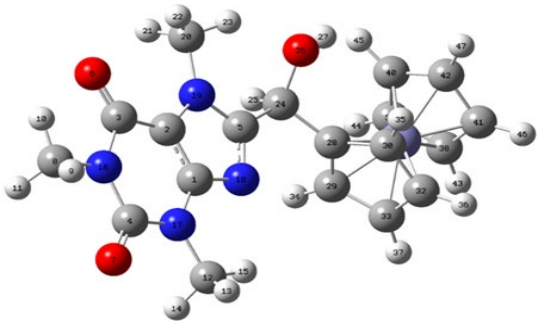

Fig. 7. FHC structure with labelled protons for ^{1}H-NMR chemical shifts prediction

Table 1: ^{1}H-NMR chemical shifts predicted by TD-DFT calculations

Shift (ppm)	Degeneracy	Atoms
5.0220460253	3	21, 22, 23
3.7524690280	1	25
3.1583410799	2	36, 37
2.9456380902	2	34, 35
2.8240369429	5	43, 44, 45, 46, 47
2.6196607598	3	13, 14, 15
2.2285051738	3	9, 10, 11
1.7769027085	1	27

It can be seen that the predicted chemical shifts can be grouped into two areas, the first is in the range of 2.22-2.94 ppm while the second from 3.15-5.02 ppm. This is in a close approximation to what has been obtained experimentally (Fig. 1). A TD-DFT calculation, at the same accuracy level, was performed to determine the UV-Vis absorption spectrum of FHC in water. The spectrum is shown in Fig. 8, which reports two maxima of absorption (λ_{max}) at 229 nm and 293 nm. As summarized in Fig. 9, the band at higher wavelengths (green arrow) is due to the HOMO-LUMO transition. Its onset is around 350 nm, corresponding to an optical band gap of 3.5 eV. The band at lower wavelengths is the result of a combination of multiple transitions (purple arrows) involving the HOMO and other higher unoccupied molecular orbitals, but also a deeper occupied orbital and the LUMO. Interestingly, all the contributions to the absorption arise from transitions involving orbitals that lay over the caffeine unit. The close approximation of the calculated UV-Vis spectrum of FHC to the experimental one (Fig. 4), which shows a λ_{max} of 302 nm in solution and 291 nm in thin film, gives an idea of the robustness of the parameters chosen for the DFT calculation.

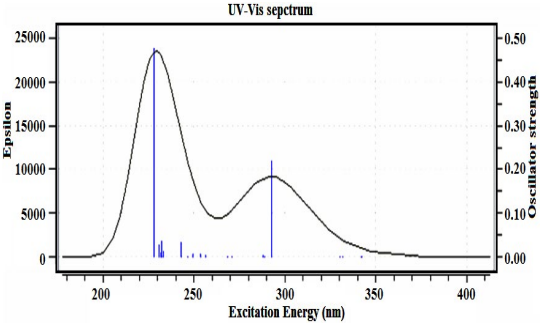

Fig. 8. UV-Vis absorption spectrum of FHC predicted by TD-DFT

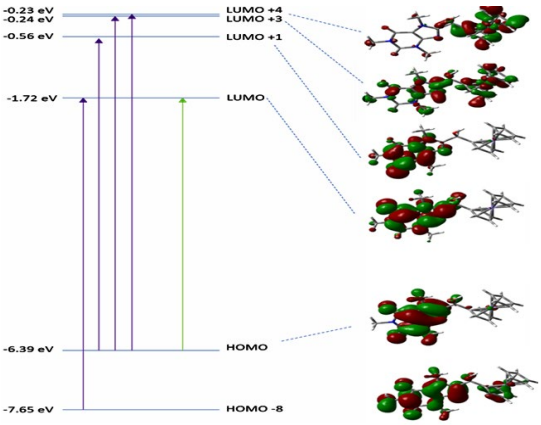

Fig. 9. Possible UV-Vis transition of FHC predicted by TD-DFT

ADME Predictions

It has become indispensable to predict the absorption, distribution, metabolism, and excretion (ADME) and drug-likeness profiles of a candidate at the early stages of drug discovery, saving considerably in terms of time and expense.[48] The most terminated candidate drugs in clinical phases are for safety and toxicity reasons rather than due to their efficacy. The behavior of FHC was investigated using two web servers, Swiss ADME .[48] As a result of the FHC, an 82.05 topological polar surface area (TPSA) was obtained, corresponding to acceptance ranges of

50.16 to 110.87. Table 2 also showed their lipophilicity and water solubility, which were all within acceptable limits. Lipinski's rule of five states that candidates' violation values should not exceed one; The FHC does not violate any drug likeness rules and has passed all tests (Table 3). Based on a permanent BBB test, FHC does not appear to have any adverse effects on the central nervous system. Moreover, it does not inhibit any essential enzymes in the cytochrome system. In addition, FHC has a high value of GI absorption. These data from Swiss ADME suggest that FHC has an ideal pharmacokinetic profile.

Table 2: Lipophilicity and water solubility of FHC

Model Name	Predicted Value	Model Name	Predicted Value
Lipophilicity		Water solubility	
Log Po/w (iLOGP)	0.00	Log S (ESOL); Solubility; Class	–3.61; 9.94e-02 mg/ml; 2.44e-04 mol/l;soluble
Log Po/w (XLOGP3)	1.79		
Log Po/w (WLOGP)	0.69	Log S (Ali); Solubility; Class	-3.13; 3.01e-01 mg/ml ; 7.38e-04 mol/lsoluble
Log Po/w (MLOGP)	2.07		
Log Po/w (SILICOS-IT)	0.07	Log S (SILICOS-IT); Solubility; Class	-0.81; 6.40e+01 mg/ml ; 1.57e-01 mol/lsoluble
Consensus Log Po/w	0.92		

Table 3: Pharmacokinetics and drug likeness of FHC compound

Model Name	Predicted Value	Model Name	Predicted Value
GI absorption	High	Log Kp (skin permeation)	-7.52 cm/s
BBB permeant	No	Lipinski	Yes; 0 violations
P-gp substrate	No	Ghose	Yes
CYP1A2 inhibitor	No	Veber	Yes
CYP2C19 inhibitor	No	Egan	Yes
CYP2C9 inhibitor	No	Muegge	Yes
CYP2D6 inhibitor	No	Bioavailability Score	0.55
CYP3A4 inhibitor	No		

Molecular docking

Molecular docking plays a significant role on drug design and discovery and has been utilized to predict binding modes between ligands and target proteins or enzymes.[49-50] The binding sites between FHC and target main protease (M^{pro}) were revealed through blind docking to shed unbiased light on the interaction by searching the entire receptor. In M^{pro}, proton transfer from the thiol of Cys 145 to the imidazole ring of His 41 activates the catalytic dyad. In the presence of a ligand, this interaction can be blocked by increasing the distance between catalytic dyads and inhibiting enzyme activity.[51-53] FHC has shown an excellent binding affinity to the active pocket of M^{pro} with a score ranging from –6.7 to –7.0 kcal/mol. The binding percentage of the conformers docked to the active site was 44%. FHC conformers formed hydrogen bonds to ASN 142 and GLU 166 with a distance range of 2.118 Å to 2.444 Å.

Figure 10 shows the interaction of FHC to the active site of M^{pro}. Our results show that the binding score energy of caffeine linked to ferrocenyl hydroxy methyl has significantly improved compared to our previously reported study on non-substituted caffeine which showed a binding score energy of –5.6 ± 0.30 kcal/mol.[18] The aforementioned residue plays a key role in the inhibition of the protease activity. Therefore, these results suggest that FHC might prevent the formation of non-structural proteins that are essential for viral replication and, therefore, the formation of new virions.

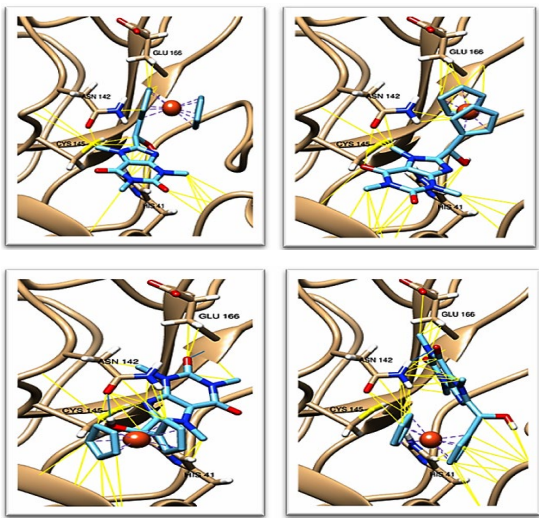

Fig. 10. The FHC conformers docked with M^{pro}, with particular attention to HIS 41, CYS 145, ASN142, and GLU 166. Nitrogen atoms are blue, oxygen atoms are red, and hydrocarbons are cyan in FHC. Blue lines depict hydrogen bonds; yellow lines represent van der Waals forces

CONCLUSION

This work presents the synthesis, DFT, and ADME predictions of a novel ferrocenyl caffeine derivative FHC, which was successfully synthesized by coupling ferrocenecarboxaldehyde to caffeine. The target compound was characterized using FT-IR, NMR, and HR-MS, and UV-Vis. A DFT calculation was carried out to gain insight into electronic and structural properties as well as the HOMO-LUMO interactions and the simulation of ^{1}H-NMR and UV-Vis spectra. The experimental and theoretical data show a good agreement. In a molecular docking study, FHC shows excellent binding affinity to M^{pro} active residues with shallow binding score energy. An in-depth investigation and discussion of FHC's interactions with M^{pro} suggest that this agent has a safe ADME profile and could be a potential inhibitor for M^{pro} of SARS-CoV-2.

ACKNOWLEDGMENT

This research was funded by the Deanship of Scientific Research, Imam Mohammad Ibn Saud Islamic University (IMSIU), Saudi Arabia, Grant Number [21-13-18-040].

Conflict of interest

The authors declare that there is no conflict of interest to be reported.

REFERENCES

1. Faudone, G.; Arifi, S.; Merk, D., The Medicinal Chemistry of Caffeine., *Journal of Medicinal Chemistry*., **2021**, *64*(11), 7156-7178.
2. Davies-Strickleton, H.; Cook, J.; Hannam, S.; Bennett, R.; Gibbs, A.; Edwards, D.; Ridden, C.; Ridden, J.; Cook, D., Assessment of the nail penetration of antifungal agents, with different physico-chemical properties. *PLOS ONE.,* **2020**, *15*(2), e0229414.
3. Wilkinson, S. C.; Maas, W. J. M.; Nielsen, J. B.; Greaves, L. C.; van de Sandt, J. J. M.; Williams, F. M., Interactions of skin thickness and physicochemical properties of test compounds in percutaneous penetration studies. *International Archives of Occupational and Environmental Health.,* **2006**, *79*(5), 405-413.
4. Lipinski, C. A.; Lombardo, F.; Dominy, B. W.; Feeney, P. J., Experimental and computational approaches to estimate solubility and permeability in drug discovery and development settings. *Advanced Drug Delivery Reviews.,* **1997**, *23*(1), 3-25.
5. Institute of Medicine Committee on Military Nutrition, R., In Caffeine for the Sustainment of Mental Task Performance: Formulations for Military Operations, National Academies Press (US). Copyright 2001 by the National Academy of Sciences. All rights reserved.: Washington (DC)., **2001**.
6. Nawrot, P.; Jordan, S.; Eastwood, J.; Rotstein, J.; Hugenholtz, A.; Feeley, M., Effects of caffeine on human health., *Food Additives & Contaminants*., **2003**, *20*(1), 1-30.
7. Magro, G., COVID-19: Review on latest available drugs and therapies against SARS-CoV-2. Coagulation and inflammation cross-talking. *Virus Research*., **2020**, *286*, 198070.
8. Rodak, K.; Kokot, I.; Kratz, E. M., Caffeine as a Factor Influencing the Functioning of the Human Body-Friend or Foe? *Nutrients*., **2021**, *13*(9).
9. Romero-Martínez, B. S.; Montaño, L. M.; Solís-Chagoyán, H.; Sommer, B.; Ramírez-Salinas, G. L.; Pérez-Figueroa, G. E.; Flores-Soto, E., Possible Beneficial Actions of Caffeine in SARS-CoV-2., *International Journal of Molecular Sciences*., **2021**, *22*(11), 5460.
10. Zhao, J.; Gonzalez, F.; Mu, D., Apnea of prematurity: from cause to treatment. *European Journal of Pediatrics.,* **2011**, *170*(9), 1097-105.
11. Welsh, E. J.; Bara, A.; Barley, E.; Cates, C. J., Caffeine for asthma. *The Cochrane Database of Systematic Reviews.,* **2010**, *2010*(1), Cd001112.
12. Baker, J. A.; McCann, S. E.; Reid, M. E.; Nowell, S.; Beehler, G. P.; Moysich, K. B., Associations Between Black Tea and Coffee Consumption and Risk of Lung Cancer Among Current and Former Smokers. *Nutrition and Cancer.,* **2005**, *52*(1), 15-21.
13. Wang, Y.; Yu, X.; Wu, Y.; Zhang, D., Coffee and tea consumption and risk of lung cancer: A dose–response analysis of observational studies. *Lung Cancer.,* **2012**, *78*(2), 169-170.
14. Yamazaki, Z.; Tagaya, I., Antiviral effects of atropine and caffeine. *The Journal of General Virology.,* **1980**, *50*(2), 429-31.

15. Shiraki, K.; Rapp, F., Effects of Caffeine on Herpes Simplex Virus. *Intervirology.,* **1988**, *29*(4), 235-240.
16. Murayama, M.; Tsujimoto, K.; Uozaki, M.; Katsuyama, Y.; Yamasaki, H.; Utsunomiya, H.; Koyama, A. H., Effect of caffeine on the multiplication of DNA and RNA viruses. *Molecular Medicine Reports.,* **2008**, *1*(2), 251-5.
17. Liu, L.; Zhang, C.; Chen, J.; Li, X., Rediscovery of Caffeine: An Excellent Drug for Improving Patient Outcomes while Fighting WARS. *Current Medicinal Chemistry*., **2021**, *28*(27), 5449-5462.
18. Elzupir, A. O., Caffeine and caffeine-containing pharmaceuticals as promising inhibitors for 3-chymotrypsin-like protease of SARS-CoV-2. *Journal of Biomolecular Structure and Dynamics.,* **2022**, *40*(5), 2113-2120.
19. Singh, A.; Lumb, I.; Mehra, V.; Kumar, V., Ferrocene-appended pharmacophores: an exciting approach for modulating the biological potential of organic scaffolds. *Dalton Transactions.,* **2019**, *48*(9), 2840-2860.
20. Peter, S.; Aderibigbe, B. A., Ferrocene-Based Compounds with Antimalaria/Anticancer Activity., *Molecules.,* **2019**, *24*(19), 3604.
21. Daeneke, T.; Kwon, T. H.; Holmes, A. B.; Duffy, N. W.; Bach, U.; Spiccia, L., High-efficiency dye-sensitized solar cells with ferrocene-based electrolytes. *Nature Chemistry*., **2011**, *3*(3), 211-15.
22. Sirbu, D.; Turta, C.; Benniston, A. C.; Abou-Chahine, F.; Lemmetyinen, H.; Tkachenko, N. V.; Wood, C.; Gibson, E., Synthesis and properties of a meso- tris–ferrocene appended zinc(ii) porphyrin and a critical evaluation of its dye sensitised solar cell (DSSC) performance. *RSC Advances*., **2014**, *4*(43), 22733-22742.
23. Kondapi, A. K.; Satyanarayana, N.; Saikrishna, A. D., A study of the Topoisomerase II activity in HIV-1 replication using the ferrocene derivatives as probes. *Archives of Biochemistry and Biophysics*., **2006**, *450*(2), 123-132.
24. Snegur, L. V., Modern Trends in Bio-Organometallic Ferrocene Chemistry. *Inorganics.,* **2022**, *10*(12), 226.
25. Aderibigbe, B. A.; Mukaya, H. E., Chapter 3-Polymer Therapeutics: Design, Application, and Pharmacokinetics. In Nano- and Microscale Drug Delivery Systems, Grumezescu, A. M., *Ed. Elsevier*., **2017**, 33-48.
26. Kealy, T. J.; Pauson, P. L., A New Type of Organo-Iron Compound. *Nature.,* **1951**, *168*(4285), 1039-1040.
27. Floris, B.; Illuminati, G.; Jones, P. E.; Ortaggi, G., The electron-donor properties of ferrocene. *Coordination Chemistry Reviews.,* **1972**, *8*(1), 39-43.
28. Astruc, D., Why is Ferrocene so Exceptional? *European Journal of Inorganic Chemistry.,* **2017**, *2017*(1), 6-29.
29. Fiorina, V. J.; Dubois, R. J.; Brynes, S., Ferrocenyl polyamines as agents for the chemoimmunotherapy of cancer. *Journal of Medicinal Chemistry.,* **1978**, *21*(4), 393-5.
30. van Staveren, D. R.; Metzler-Nolte, N., Bioorganometallic Chemistry of Ferrocene. *Chemical Reviews.,* **2004**, *104*(12), 5931-5986.
31. Hillard, E. A.; Vessières, A.; Jaouen, G., Ferrocene Functionalized Endocrine Modulators as Anticancer Agents. In Medicinal Organometallic Chemistry, Jaouen, G.; Metzler-Nolte, N., Eds. *Springer Berlin Heidelberg: Berlin, Heidelberg*., **2010**, 81-117.
32. Peter, S.; Aderibigbe, B. A. Ferrocene-Based Compounds with Antimalaria/Anticancer Activity Molecules [Online]., **2019**.
33. Khalaf, M. M.; El-Lateef, H. M. A.; Alhadhrami, A.; Sayed, F. N.; Mohamed, G. G.; Gouda, M.; Shaaban, S.; Abu-Dief, A. M., Synthesis, Spectroscopic, Structural and Molecular Docking Studies of Some New Nano-Sized Ferrocene-Based Imine Chelates as Antimicrobial and Anticancer Agents. *Materials.,* **2022**, *15*(10), 3678.
34. Larik, F. A.; Saeed, A.; Fattah, T. A.; Muqadar, U.; Channar, P. A., Recent advances in the synthesis, biological activities and various applications of ferrocene derivatives. *Applied Organometallic Chemistry.,* **2017**, *31*(8), e3664.
35. Poje, G.; Marinovi, M.; Pavi, K.; Mio, M.; Kralj, M.; de Carvalho, L. P.; Held, J.; Perkovi, I.; Raji, Z., Harmicens, Novel Harmine and Ferrocene Hybrids: Design, Synthesis and Biological Activity. *International Journal of Molecular Sciences.,* **2022**, *23*(16), 9315.
36. Fouda, M. F. R.; Abd-Elzaher, M. M.; Abdelsamaia, R. A.; Labib, A. A., On the medicinal chemistry of ferrocene. *Applied Organometallic Chemistry.,* **2007**, *21*(8), 613-625.

37. Ludwig, B. S.; Correia, J. D. G.; Kühn, F. E., Ferrocene derivatives as anti-infective agents. *Coordination Chemistry Reviews.,* **2019**, *396*, 22-48.
38. Gama, N.; Kumar, K.; Ekengard, E.; Haukka, M.; Darkwa, J.; Nordlander, E.; Meyer, D., Gold(I) complex of 1,1λbis(diphenylphosphino) ferrocene–quinoline conjugate: a virostatic agent against HIV-1. *BioMetals.,* **2016**, *29*(3), 389-397.
39. Kondapi, A. K.; Satyanarayana, N.; Saikrishna, A. D., A study of the topoisomerase II activity in HIV-1 replication using the ferrocene derivatives as probes. *Arch Biochem Biophys.,* **2006**, *450*(2), 123-32.
40. Hu, B.; Guo, H.; Zhou, P.; Shi, Z.-L., Characteristics of SARS-CoV-2 and COVID-19. *Nature Reviews Microbiology.,* **2021**, *19*(3), 141-154.
41. Samrat, S. K.; Tharappel, A. M.; Li, Z.; Li, H., Prospect of SARS-CoV-2 spike protein: Potential role in vaccine and therapeutic development. *Virus Research.,* **2020**, *288*, 198141.
42. Pillaiyar, T.; Manickam, M.; Namasivayam, V.; Hayashi, Y.; Jung, S.-H., An Overview of Severe Acute Respiratory Syndrome–Coronavirus (SARS-CoV) 3CL Protease Inhibitors: Peptidomimetics and Small Molecule Chemotherapy. *Journal of Medicinal Chemistry.,* **2016**, *59*(14), 6595-6628.
43. Heo, Y.-A.; Deeks, E. D., Sofosbuvir/ Velpatasvir/Voxilaprevir: *A Review in Chronic Hepatitis C. Drugs.,* **2018**, *78*(5), 577-587.
44. Chopp, S.; Vanderwall, R.; Hult, A.; Klepser, M., Simeprevir and sofosbuvir for treatment of hepatitis C infection. *American Journal of Health-System Pharmacy.,* **2015**, *72*(17), 1445-1455.
45. Kanters, S.; Socias, M. E.; Paton, N. I.; Vitoria, M.; Doherty, M.; Ayers, D.; Popoff, E.; Chan, K.; Cooper, D. A.; Wiens, M. O.; Calmy, A.; Ford, N.; Nsanzimana, S.; Mills, E. J., Comparative efficacy and safety of second-line antiretroviral therapy for treatment of HIV/AIDS: a systematic review and network meta-analysis. *The Lancet HIV.,* **2017**, *4*(10), e433-e441.
46. Elzupir, A. O., Molecular Docking and Dynamics Investigations for Identifying Potential Inhibitors of the 3-Chymotrypsin-like Protease of SARS-CoV-2: Repurposing of Approved Pyrimidonic Pharmaceuticals for COVID-19 Treatment. *Molecules.,* **2021**, *26* (24).
47. M. J. Frisch, G. W. T., H. B. Schlegel, G. E. Scuseria, M. A. Robb, J. R. Cheeseman, G. Scalmani, V. Barone, G. A. Petersson, H. Nakatsuji, X. Li, M. Caricato, A. Marenich, J. Bloino, B. G. Janesko, R. Gomperts, B. Mennucci, H. P. Hratchian, J. V. Ortiz, A. F. Izmaylov, J. L. Sonnenberg, D. Williams-Young, F. Ding, F. Lipparini, F. Egidi, J. Goings, B. Peng, A. Petrone, T. Henderson, D. Ranasinghe, V. G. Zakrzewski, J. Gao, N. Rega, G. Zheng, W. Liang, M. Hada, M. Ehara, K. Toyota, R. Fukuda, J. Hasegawa, M. Ishida, T. Nakajima, Y. Honda, O. Kitao, H. Nakai, T. Vreven, K. Throssell, J. A. Montgomery, Jr., J. E. Peralta, F. Ogliaro, M. Bearpark, J. J. Heyd, E. Brothers, K. N. Kudin, V. N. Staroverov, T. Keith, R. Kobayashi, J. Normand, K. Raghavachari, A. Rendell, J. C. Burant, S. S. Iyengar, J. Tomasi, M. Cossi, J. M. Millam, M. Klene, C. Adamo, R. Cammi, J. W. Ochterski, R. L. Martin, K. Morokuma, O. Farkas, J. B. Foresman, and D. J. , Gaussian 09, Revision A.02. **2016**.
48. Sitkowski, J.; Stefaniak, L.; Nicol, L.; Martin, M. L.; Martin, G. J.; Webb, G. A., Complete assignments of the 1H, 13C and 15N NMR spectra of caffeine. Spectrochimica Acta Part A: *Molecular and Biomolecular Spectroscopy.,* **1995**, *51*(5), 839-841.
49. Morris, G. M.; Lim-Wilby, M., Molecular docking. *Methods in molecular biology (Clifton, N.J.).*, **2008**, *443*, 365-82.
50. Kumar, S.; Saini, V.; Maurya, I. K.; Sindhu, J.; Kumari, M.; Kataria, R.; Kumar, V., Design, synthesis, DFT, docking studies and ADME prediction of some new coumarinyl linked pyrazolylthiazoles: Potential standalone or adjuvant antimicrobial agents. *PLoS One.,* **2018**, *13*(4), e0196016.
51. Banerjee, S., An insight into the interaction between α-ketoamide-based inhibitor and coronavirus main protease: A detailed in silico study. *Biophysical Chemistry.*, **2021**, *269*, 106510.
52. Ramos-Guzmán, C. A.; Ruiz-Pernía, J. J.; Tuñón, I., Inhibition Mechanism of SARS-CoV-2 Main Protease with Ketone-Based Inhibitors Unveiled by Multiscale Simulations: Insights for Improved Designs*. *Angewandte Chemie (International ed. in English).*, **2021**, *60*(49), 25933-25941.
53. Ramos-Guzmán, C. A.; Ruiz-Pernía, J. J.; Tuñón, I., Multiscale Simulations of SARS-CoV-2 3CL Protease Inhibition with Aldehyde Derivatives. Role of Protein and Inhibitor Conformational Changes in the Reaction Mechanism. *ACS Catalysis.,* **2021**, *11*(7), 4157-4168.